General entire-domain method for analysis of dielectric scatterers

B.M.Notaroš
B.D.Popović

Indexing terms: Galerkin solutions, Lossy scatterers, Dielectric scatterers

Abstract: A novel, entire-domain method is proposed for the analysis of dielectric scatterers of arbitrary geometry, made of an inhomogeneous lossy dielectric. The scatterer is modelled by arbitrarily large trilinear hexahedrons. Each trilinear hexahedron is completely defined by its eight vertices, which can be positioned in space arbitrarily. The equivalent electric displacement vector is approximated by 3D polynomials in local (generally nonorthogonal) co-ordinates satisfying automatically the continuity condition for its normal component over shared sides of hexahedrons. The unknown current coefficients are determined by a Galerkin solution of the volume two-potential integral equation. The method is very accurate, efficient and reliable, enabling the analysis of up to electrically medium-sized dielectric scatterers on even standard PCs. Numerical results are in excellent agreement with the results obtained by available methods. However, the proposed method requires fewer unknowns (for at least an order of magnitude), and consequently very much reduced CPU time when compared with the existing, subdomain methods.

1 Introduction

Numerical analysis of (lossy) dielectric scatterers is an important problem of applied electromagnetics. It is required in the analysis of electromagnetic systems that include dielectric bodies. Subdomain methods founded on numerical solution of volume integral equations are widely used for the analysis of dielectric scatterers of arbitrary shape and inhomogeneity of up to medium electrical size [1–7]. According to these methods, the scatterer volume is modelled by electrically small elements (cubes, parallelepipeds, tetrahedrons or polyhedrons), with low-order basis functions (3D pulses, 3D rooftop functions or 3D linear functions) for the approximation of current (or field) inside them. This results in a very large number of unknowns to be determined. Consequently, serious problems are frequently encountered concerning computer memory requirements and the necessary computing time. These problems are present also with (metallic) wires and plates, but they become particularly pronounced in the case of volume-penetrable scatterers.

Relatively recently, we proposed an entire-domain method for the analysis of arbitrary dielectric scatterers of medium electrical size [8]. According to this method the scatterer is approximated by a system of arbitrarily large right parallelepipeds in which the total current density vector was approximated by three-dimensional simple power functions in local orthogonal Cartesian coordinates. The volume EFIE was solved by point matching.

In this paper a novel, general entire-domain moment method is proposed for the analysis of possibly inhomogeneous and lossy dielectric scatterers that can exceed medium electrical size. In a sense, it represents a generalisation of the method presented in [8] but it is significantly more accurate, efficient and flexible. The starting equation is the volume two-potential integral equation, and the unknown is the equivalent electric displacement vector whose normal component is continuous on any boundary surface. The approximation of scatterer geometry is performed by means of so-called trilinear hexahedrons. This is a body with straight edges and curved sides, defined uniquely by its eight vertices, which can be positioned in space completely arbitrarily. The hexahedrons, theoretically, may be of arbitrary electrical size. The equivalent displacement vector is approximated by extremely flexible entire-domain three-dimensional power series in local co-ordinates. The basis functions are constructed which satisfy automatically the continuity condition for the normal component of the displacement vector on adjacent surfaces of hexahedrons. This results in additional reduction in the number of unknowns, and prevents fictitious surface charges appearing in the numerical solution on surfaces shared by any two hexahedrons across which the properties of the dielectric are continuous functions. The unknown coefficients are determined by the Galerkin method, and the two-potential equation is transformed into a form which does not require numerical differentiation. Very efficient and accurate procedures have been devised for the evaluation of the resulting Galerkin impedances.

The results obtained by the proposed method are compared with the existing results obtained by the subdomain approach, indicating high accuracy of the

IEE Proceedings online no. 19960695

Paper first received 4th December 1995 and in final revised form 20th June 1996

The authors are with the Department of Electrical Engineering, University of Belgrade, PO Box 816, 11001 Belgrade, Yugoslavia

proposed method and, in particular, the possibility of analysing relatively large scatterers by personal computers, in a very reasonable amount of CPU time. When compared with available (subdomain) methods, the novel, entire-domain method requires much less unknowns (for one and even two orders of magnitude). Of course, the dependence of the required CPU time T on the number of unknowns N differs significantly from one method to another. For the present method, as for all classical moment methods [9], it is of the form $T(N) = AN^2 + BN^3$ (A and B are constants). On the other hand, some subdomain techniques, based on using the conjugate gradient method and the fast Fourier transform (FFT) [3, 6, 7], make the function $T(N)$ to increase much more slowly with increasing N than $AN^2 + BN^3$. Nevertheless, since $N_{subdomain}$ always greatly exceeds $N_{entire\ domain}$, in all cases considered by the authors (some of which are presented in this paper) the overall CPU time needed for solving the same problem with approximately equal accuracy strongly favours the present method over all subdomain methods.

2 Volume integral equation for dielectric scatterer

Consider a dielectric body of arbitrary shape and inhomogeneity situated in a vacuum in a time-harmonic incident field of complex electric field intensity $\mathbf{E}_i$ and angular frequency ω. Let relative permittivity ε_r of the scatterer and its conductivity σ be known functions of position, and let at all points permeability be μ_0. The total (polarisation plus conduction) induced volume current-density vector $\mathbf{J}$ at any point of the scatterer is given by

$$\mathbf{J} = j\omega(\varepsilon_e - \varepsilon_0)(\mathbf{E}_i + \mathbf{E}), \quad \varepsilon_e = \varepsilon - j\sigma/\omega = \varepsilon_{er}\varepsilon_0 \tag{1}$$

where ε_e is the equivalent complex permittivity of the dielectric, and $\mathbf{E}$ is the field due to induced currents and charges (the secondary field). The total (polarisation plus free) induced volume and surface charge densities ρ and ρ_s are connected with $\mathbf{J}$ by the continuity equation and the corresponding boundary condition

$$\rho = \frac{j}{\omega}\mathrm{div}\mathbf{J}, \quad \rho_s = \frac{j}{\omega}\mathbf{n}\cdot(\mathbf{J}_1 - \mathbf{J}_2) \tag{2}$$

where the unit vector $\mathbf{n}$, normal to the surface with surface charges (the surface of discontinuity of ε_e), is directed into medium 1.

The Lorentz potentials of the secondary field are computed as ($\mathbf{r}$ is the position vector of the field point, and $\mathbf{r}'$ of the source point)

$$\mathbf{A}(\mathrm{r}) = \mu_0 \int_V \mathbf{J}(\mathbf{r}')g(\mathbf{r},\mathbf{r}')dV \tag{3}$$

$$\Phi(\mathbf{r}) = \frac{1}{\varepsilon_0}\int_V \rho(\mathbf{r}')g(\mathbf{r},\mathbf{r}')dV + \frac{1}{\varepsilon_0}\int_{S_d} \rho_s(\mathbf{r}')g(\mathbf{r},\mathbf{r}')dS \tag{4}$$

Here, V is the domain of the body, S_d are surfaces of discontinuity in ε_e, and g is the free-space Green's function

$$g(\mathbf{r},\mathbf{r}') = \frac{\mathrm{e}^{-j\beta_0 R}}{4\pi R}, \quad R = |\mathbf{r}-\mathbf{r}'|, \quad \beta_0 = \omega\sqrt{\varepsilon_0\mu_0} = 2\pi/\lambda_0 \tag{5}$$

We shall see that, provided that appropriate functions are adopted for the approximation of current, it is numerically much more convenient to substitute $\mathbf{J}$ as the unknown by the equivalent electric displacement vector, defined by

$$\mathbf{D} = \varepsilon_e(\mathbf{E}_i + \mathbf{E}) = \mathbf{J}/(j\omega K), \quad K = \frac{\varepsilon_e - \varepsilon_0}{\varepsilon_e} \tag{6}$$

where the parameter K is usually termed the electric contrast. It is a simple matter to show that, at all surfaces of discontinuity in ε_e, $\mathbf{n}\cdot\mathbf{D}_1 = \mathbf{n}\cdot\mathbf{D}_2$.

By combining eqns. 1–6, and having in mind that $\mathbf{E} = -j\omega\mathbf{A} - \mathrm{grad}\Phi$, we obtain the volume two-potential integral equation, with $\mathbf{D}(\mathbf{r}')$ as the single unknown,

$$\frac{\mathbf{D}(\mathbf{r})}{\varepsilon_e(\mathbf{r})} + j\omega\mathbf{A}(\mathbf{r}) + \mathrm{grad}\Phi(\mathbf{r}) = \mathbf{E}_i(\mathbf{r}) \tag{7}$$

where $\mathbf{r}$ is the position vector of an arbitrary point inside the dielectric body.

3 Numerical solution for volume current distribution

In this Section we propose a general numerical solution of eqn. 7, based on the method of moments [9].

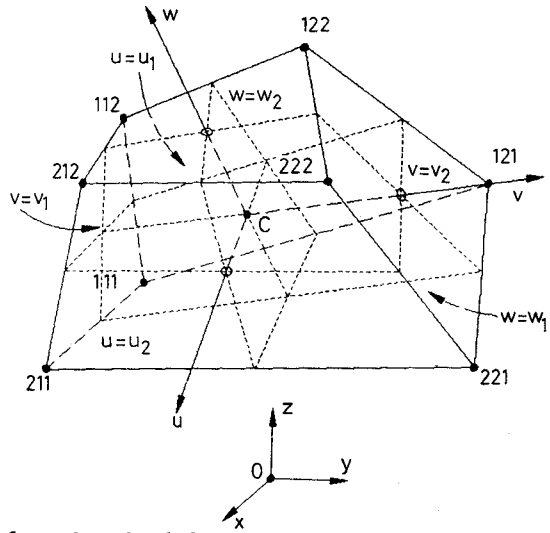

Fig. 1 *Trilinear hexahedron*

As the basic element for modelling the geometry of dielectric scatterers of arbitrary shape and inhomogeneity, we use a geometrical body sketched in Fig. 1 [10]. This body is determined solely by eight arbitrary points in space, which represent its vertices, just as a tetrahedron is determined uniquely by the position of its four vertices. In the adopted local u-v-w co-ordinate system indicated in Fig. 1, it is defined by the following parametric equation:

$$\begin{aligned}\mathbf{r}(u,v,w) = \frac{1}{\Delta u\Delta v\Delta w}[&-(u-u_2)(v-v_2)(w-w_2)\mathbf{r}_{111}\\ &+(u-u_2)(v-v_2)(w-w_1)\mathbf{r}_{112}\\ &+(u-u_2)(v-v_1)(w-w_2)\mathbf{r}_{121}\\ &-(u-u_2)(v-v_1)(w-w_1)\mathbf{r}_{122}\\ &+(u-u_1)(v-v_2)(w-w_2)\mathbf{r}_{211}\\ &-(u-u_1)(v-v_2)(w-w_1)\mathbf{r}_{212}\\ &-(u-u_1)(v-v_1)(w-w_2)\mathbf{r}_{221}\\ &+(u-u_1)(v-v_1)(w-w_1)\mathbf{r}_{222}]\end{aligned}$$

$$\text{with } \Delta u = u_2 - u_1, \quad \Delta v = v_2 - v_1, \quad \Delta w = w_2 - w_1 \tag{8}$$

In this equation, u_1 and u_2, v_1 and v_2, and w_1 and w_2 are arbitrary starting and end local co-ordinates defining the sides of the body, and $\mathbf{r}$ is the position vector of the point inside the body corresponding to the co-ordinates

u, v and w with respect to the global origin O. The vectors $\mathbf{r}_{ijk}$, $i = 1, 2, j = 1, 2, k = 1, 2$, are the position vectors of the eight body vertices. Dotted lines indicate parts of some co-ordinate lines. The body edges and all co-ordinate lines are straight, while its sides (and all co-ordinate surfaces) are generally curved. Such a body we term the trilinear hexahedron. Note that the trilinear hexahedron sides (so-called bilinear quadrilaterals) cannot be concave or convex, but only inflected (which is a single moderate disadvantage of this model). Note also that, in the general case, the parametric coordinate system u-v-w in which a trilinear hexahedron is defined is not orthogonal, and the u, v and w co-ordinates are not length co-ordinates.

After elementary transformations, eqn. 8 can be rewritten as

$$\begin{aligned}\mathbf{r}(u,v,w) =& \mathbf{r}_c + \mathbf{r}_u u + \mathbf{r}_v v + \mathbf{r}_w w \\ &+ \mathbf{r}_{uv} uv + \mathbf{r}_{uw} uw + \mathbf{r}_{vw} vw + \mathbf{r}_{uvw} uvw \\ & u_1 \le u \le u_2, \quad v_1 \le v \le v_2, \quad w_1 \le w \le w_2\end{aligned} \tag{9}$$

where $\mathbf{r}_c$, $\mathbf{r}_u$, $\mathbf{r}_v$, $\mathbf{r}_w$, $\mathbf{r}_{uv}$, $\mathbf{r}_{uw}$, $\mathbf{r}_{vw}$ and $\mathbf{r}_{uvw}$ are constant vectors that can be expressed in terms of the position vectors of the hexahedron vertices and the boundary parametric coordinates.

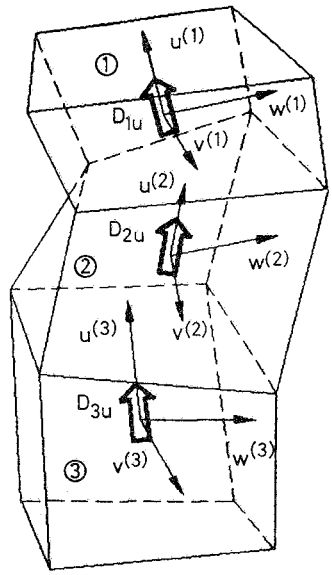

Fig. 2 *Three trilinear hexahedrons in a chain*

Imagine a geometrical model of a body constructed from several trilinear hexahedrons. Consider any three hexahedrons in this model which are connected in a chain, as shown in Fig. 2. The vector $\mathbf{D}$ in each trilinear hexahedron we decompose into three local components $\mathbf{D} = \mathbf{D}_u + \mathbf{D}_v + \mathbf{D}_w$. For simplicity, the local co-ordinate systems in the hexahedrons are oriented in the same way. Assume also that the starting values of the parametric co-ordinates equal to -1, and the end values to $+1$, in all the hexahedrons. The unknown function $\mathbf{D}_u$ in every hexahedron we initially represent as

$$\mathbf{D}_u = \frac{1}{\xi}\frac{d\Psi_u}{dvdw}\frac{\partial \mathbf{r}}{\partial u}, \quad \xi = \frac{\partial \mathbf{r}}{\partial u}\cdot\left(\frac{\partial \mathbf{r}}{\partial v}\times\frac{\partial \mathbf{r}}{\partial w}\right) \tag{10}$$

where $d\Psi_u$ is the flux of vector $\mathbf{D}_u$ through the surface of an infinitesimal parallelogram, the sides of which are along the v- and w-co-ordinate line at the point (u,v,w), and $\mathbf{r}$ is given in eqn. 9.

It is not difficult to prove that the continuity condition for the normal component of vector $\mathbf{D}$, $D_{1u}\cos\gamma_1 = D_{2u}\cos\gamma_2 = (D_u)_{norm}$ (see Fig. 3), can be satisfied automatically by introducing the following entire-domain power series for any trilinear hexahedron:

$$\frac{d\Psi_u}{dvdw} = \sum_{i=0}^{N_u}\sum_{j=0}^{N_v}\sum_{k=0}^{N_w} a_{uijk} v^j w^k \begin{Bmatrix} (1-u), & i=0 \\ (u+1), & i=1 \\ (u^i-1), & i=2,4,\ldots,N_u(2) \\ (u^i-u), & i=3,5,\ldots,N_u(2) \end{Bmatrix}, \quad -1 \le u,v,w \le 1 \tag{11}$$

Here, N_u, N_v and N_w are the adopted degrees of the polynomials, and a_{uijk} are unknown complex coefficients. The expansions analogous to those in eqns. 10 and 11 are adopted for the components D_v and D_w. Since the degrees N_u, N_v and N_w can be arbitrarily large, the hexahedrons in the geometrical model can, in principle, be of any electrical size allowed by the geometry and the electrical properties of the body (the entire-domain nature of the proposed method). Of course, the electrical size of a body is limited by the possibilities of the computer used for the analysis.

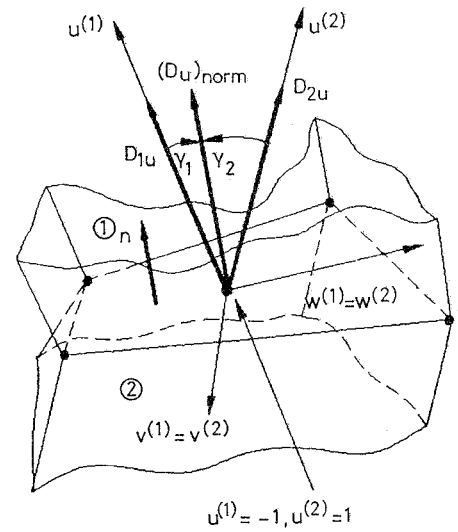

Fig. 3 *Enlarged detail of the boundary surface between hexahedrons 1 and 2 in Fig. 2*

In the expansion in eqn. 11, the functions $(1-u)v^j w^k$ and $(u+1)v^j w^k$ serve for the adjustment of the boundary condition for vector $\mathbf{D}$ on boundary surfaces (see, for example, the boundary surfaces 1–2 and 2–3 in Fig. 2). With this, certain number of the coefficients a_{uijk} (where $i = 0$ or 1) is the same for any two adjacent hexahedrons, and the total number of unknowns for a problem is reduced significantly. In addition, theoretically nonexistent surface charges at a boundary surface of any two hexahedrons across which the properties of the dielectric are continuous functions cannot be obtained as a consequence of inaccurate numerical solution of a problem. This is particularly important when using lower-order current approximations. Finally, since the vector $\mathbf{D}$ in the air is not considered as unknown, the boundary condition for $\mathbf{D}_{norm}$ on the surface dielectric/air is not adjusted automatically but numerically.

Now concentrate on an arbitrary trilinear hexahedron in the geometrical model of a scatterer (e.g. that in Fig. 1). Assume for simplicity that the dielectric inside it is homogeneous, of electrical contrast K, and that the vector $\mathbf{D}$ inside it has only the u-component, $\mathbf{D} = \mathbf{D}_u$. After extensive transformations, one obtains the following integral expressions for the potentials $\mathbf{A}$ and Φ owing to currents and charges inside the hexahedron, at a field point defined by the position vector $\mathbf{r}_0$:

$$\mathbf{A}(\mathbf{r}_0) = j\omega\mu_0 K \int_{u_1}^{u_2}\int_{v_1}^{v_2}\int_{w_1}^{w_2} \frac{d\Psi_u}{dvdw}\frac{\partial \mathbf{r}}{\partial u} g(\mathbf{r}_0, \mathbf{r}) dudvdw \quad (12)$$

$$\Phi(\mathbf{r}_0) = \frac{1}{\varepsilon_0}\left[-K\int_{u_1}^{u_2}\int_{v_1}^{v_2}\int_{w_1}^{w_2}\frac{\partial}{\partial u}\left(\frac{d\Psi_u}{dvdw}\right) g(\mathbf{r}_0, \mathbf{r}) dudvdw + \sum_{p=1}^{2}(-1)^p \Delta K_p \int_{v_1}^{v_2}\int_{w_1}^{w_2} \left.\frac{d\Psi_u}{dvdw}\right|_{u=u_p} g(\mathbf{r}_0, \mathbf{r}_p) dvdw\right] \quad (13)$$

In these equations $\mathbf{r}$ is the position vector of a source point inside the hexahedron given in eqn. 9, while $\mathbf{r}_p$ is the position vector of a source point belonging to a bilinear quadrilateral defined by $u = u_p$ (p = 1 or 2). ΔK_p represents the difference in electrical contrast of the adjacent hexahedrons (see, for example, Fig. 2), $\Delta K_p = K - K_p$, where K_p is the electrical contrast of the hexahedron a side of which coincides with the side of the hexahedron considered defined by $u = u_p$ (p = 1 or 2).

For the determination of the unknown current-distribution coefficients, $[a]$, defined in eqn. 11, we adopt the Galerkin method. It implies an additional volume integration of the integral equation (eqn. 7), resulting in the following equation:

$$\langle \mathbf{f}_m, \frac{\mathbf{D}}{\varepsilon_e}\rangle + j\omega\langle \mathbf{f}_m, \mathbf{A}\rangle + \langle \mathbf{f}_m, \mathrm{grad}\Phi\rangle = \langle \mathbf{f}_m, \mathbf{E}_i\rangle \quad (14)$$

In this equation, $\langle \mathbf{f}_m, \mathbf{E}\rangle$ is the inner scalar product over the volume V_m of the mth trilinear hexahedron in the geometrical model of the scatterer, and $\mathbf{f}_m$ is the weighting (testing) function defined in that hexahedron, multiplied by the corresponding unit vector. To avoid numerical differentiation implied in gradΦ, the third term in eqn. 14 can be transformed by expanding div($\mathbf{f}_m\Phi$) and applying the divergence theorem. Thus from eqn. 14 we obtain the following equation:

$$\int_{V_m} \mathbf{f}_m \cdot \frac{\mathbf{D}}{\varepsilon_e} dV_m + j\omega \int_{V_m} \mathbf{f}_m \cdot \mathbf{A} dV_m - \int_{V_m} \Phi \mathrm{div}\mathbf{f}_m dV_m + \oint_{S_m} \Phi \mathbf{f}_m \cdot d\mathbf{S}_m = \int_{V_m} \mathbf{f}_m \cdot \mathbf{E}_i dV_m \quad (15)$$

Here, S_m is the boundary surface of the mth trilinear hexahedron. This equation represents a modified version of the volume two-potential integral equation (with the vector $\mathbf{D}$ as the unknown) which does not require numerical differentiation. The potentials $\mathbf{A}$ and Φ in the resulting expressions for the Galerkin impedances (i.e. the system matrix elements) are evaluated on the basis of eqns. 12 and 13, while the electric-field intensity vector $\mathbf{E}$, of course, is not necessary to evaluate. A rather complicated, but very efficient and accurate, procedure has been developed for the evaluation of the impedances [10], but owing to lack of space it is not elaborated here. The final system of linear equations we solve by the Gaussian elimination method.

The present method can in principle normally handle the scatterers which contain conductors, i.e. the dielectrics with $\sigma >> \omega\varepsilon$. According to our experience, however, the analysis based on the present method can in such cases be made much more accurate and efficient if the thin-wall model of a conducting body is introduced, with the wall thickness of the order of a skin depth. Of course, such walls are modelled also by trilinear hexahedrons.

4 Numerical results

All numerical results obtained by the proposed method which are presented below were obtained on a PC-486/66MHz (8Mbyte DRAM). In all the examples the number of unknowns N_{unkn} and the total CPU time T_{CPU} are given to make easier the comparison with the efficiency of other methods. N_{el} denotes the number of elements (trilinear hexahedrons) used for modelling the scatterer.

In all the examples the origin of the global cartesian x-y-z co-ordinate system is adopted to be at the centre of the scatterer. In the cases of scatterers with the shape of a parallelepiped the cartesian co-ordinate axes are set parallel to the scatterer edges. In such cases, the local parametric u-, v- and w-axis we adopt to be parallel to the global x-, y- and z-axis, respectively. For scatterers with curved surfaces the geometrical model was always constructed so that the surface of the model approximated the scatterer surface in the best possible manner, with the condition that the volume of the model and the volume of the scatterer be the same.

Consider first a homogeneous lossless dielectric cube of relative permittivity $\varepsilon_r = 9$ situated in an incident plane electromagnetic wave of the electric-field intensity $\mathbf{E}_i = 377\exp(-j\beta_0 z)\,\mathbf{i}_x$ V/m. Let the cube edge length be $a = \lambda_0/5 = 3\lambda_d/5$, where λ_d represents the wavelength in the dielectric. The cube can be modelled exactly by a single trilinear hexahedron ($N_{el} = 1$). The degrees of the polynomial approximation adopted were $N_u = N_v = N_w = 2$, but the number of unknowns was reduced by reducing the degree of approximation for individual components of the vector $\mathbf{D}$ in directions transversal to that component for $\Delta N_{tran} = 1$. For example, the highest-degree term in the approximation for the D_u component was adopted to be $(u^2 - 1)vw$ [see eqn. 11]. With this, the number of unknowns amounted to only $N_{unkn} = 36$ ($T_{CPU} = 4.39$s).

Shown in Fig. 4 is the scattered far field in planes $\phi = 0°$ and $\phi = 90°$, normalised with respect to its maximal value. The results are compared with those obtained by four different subdomain methods: (i) method [4] (volume formulation, 1536 unknowns); (ii) method [4] (surface formulation, 576 unknowns); (iii) method [5] (about 4600 unknowns); and (iv) method [7] (1176 unknowns, T_{CPU} = 304s on a VAX 3100/76 workstation). From the Figure we see excellent agreement of the results obtained by the proposed method with those obtained by subdomain methods (ii)–(iv). Discrepancies of the results obtained by subdomain method (i) can be explained by insufficient quality of the pulse approximation and the resulting errors due to the appearance of actually nonexistent surface charges on the small cube sides. Note that the ratio of the number of unknowns used in the four cited

subdomain methods and that required by the proposed method is about 42, 16, 120 and 32, respectively.

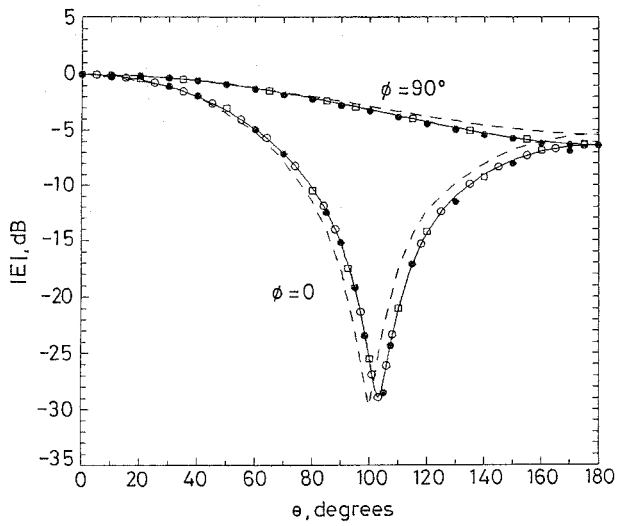

Fig. 4 *Normalised scattered far-field 20 log $|E/E_{max}|$ for homogeneous lossless cubical dielectric scatterer in planes $\phi = 0°$ and $\phi = 90°$*
Cube edge length a = $\lambda_0/5$; $\varepsilon_r = 9$; $\mathbf{E}_i = 377\exp(-j\beta_0 z)\mathbf{i}_x$ V/m
——— this method, 36 unknowns
– – – method [4] (volume formulation), 1536 unknowns
• • • method [4] (surface formulation), 576 unknowns
○ ○ ○ method [5], about 4600 unknowns
□ □ □ method [7], 1176 unknowns

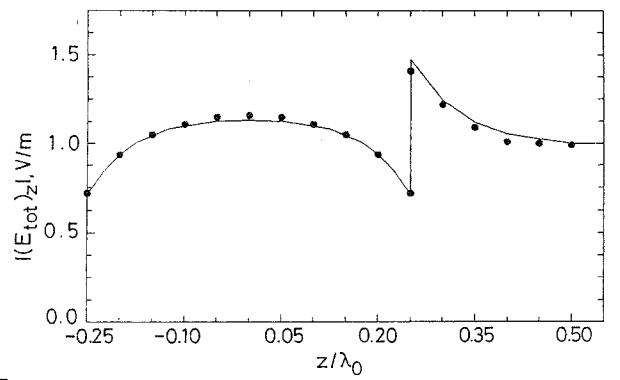

Fig. 5 *Total electric field inside and close to lossless dielectric cylindrical scatterer of square cross-section of area $(0.015\lambda_0)^2$ and length $l = \lambda_0/2$ along scatterer axis*
$\varepsilon_r = 2$; $\mathbf{E}_i = 1\exp(-j\beta_0 x)\mathbf{i}_z$ V/m (TM incidence)
——— this method, 11 unknowns
• • • method [3], 768 unknowns

As the next example, consider a homogeneous lossless thin dielectric cylinder of finite length l and square cross-section of square side $a = 0.03l$. Assume that the incident plane wave E-field is parallel to the cylinder axis (TM incidence), and that $\mathbf{E}_i = 1\exp(-j\beta_0 x)\mathbf{i}_z$ V/m, $\varepsilon_r = 2$ and $l = \lambda_0/2 \simeq 0.707\lambda_d$. In the analysis by the proposed method, it was adopted that $N_{el} = 1$, $N_u = N_v = 1$ and $N_w = 2$, with the parameter ΔN_{tran} (defined in the preceding example) equal to $\Delta N_{tran} = 1$. In that case $N_{unkn} = 11$ and $T_{CPU} = 1.54$s.

Fig. 5 shows the distribution of the total (incident plus secondary) electric field $\mathbf{E}_{tot}$ inside and in the vicinity of the cylindrical scatterer, along the scatterer axis. The results obtained by the proposed method are compared with those from [3]. Excellent agreement is observed between the two sets of results, but note that the present method requires only 11 unknowns, while the other method needs 768 unknowns.

Fig. 6 shows normalised bistatic cross-section S_{bist}/λ_0^2 of a homogeneous lossless sphere with $\varepsilon_r = 2$, in planes $\phi = 0°$ and $\phi = 90°$. The sphere is excited by a plane wave with $\mathbf{E}_i = 1\exp(-j\beta_0 z)\mathbf{i}_x$ V/m. Its radius a is given as $\beta_0 a = 1$ ($2a = 0.45\lambda_d$). The sphere is approximated

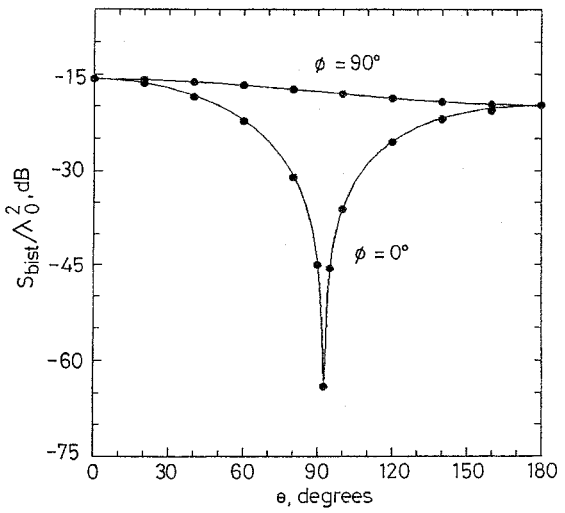

Fig. 6 *Normalised bistatic cross-section $10\log(S_{bist}/\lambda_0^2)$ of homogeneous lossless dielectric sphere for various θ in planes $\phi = 0°$ and $\phi = 90°$*
Radius a given by $\beta_0 a = 1$; $\varepsilon_r = 2$; $\mathbf{E}_i = 1\exp(-j\beta_0 z)\mathbf{i}_x$ V/m
——— this method, 27 elements, 208 unknowns
• • • analytical solution, Mie's series [11]

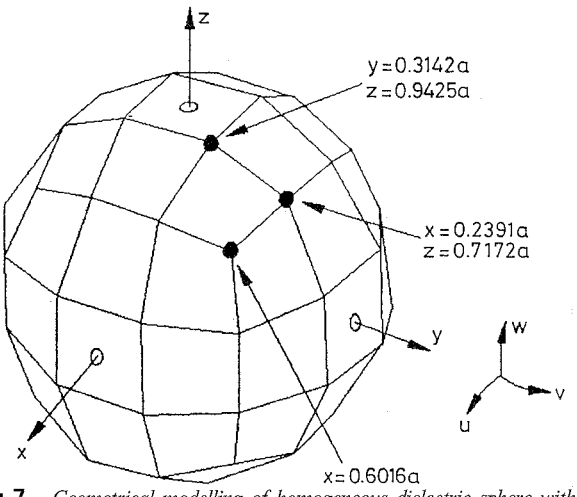

Fig. 7 *Geometrical modelling of homogeneous dielectric sphere with 27 trilinear hexahedrons*
Sphere surface is first approximated by 54 bilinear quadrilaterals

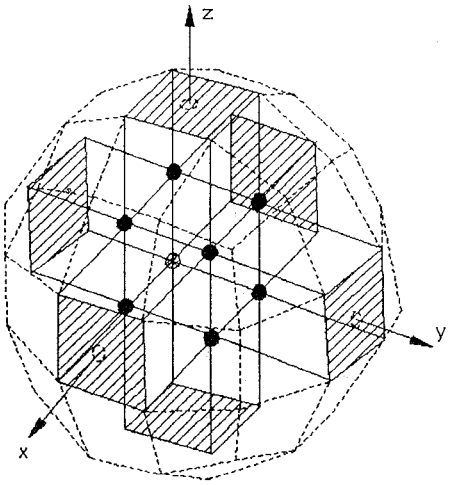

Fig. 8 *Geometrical modelling of homogeneous dielectric sphere with 27 trilinear hexahedrons*
Sphere volume is then divided into 27 parts

by $N_{el} = 3 \times 3 \times 3 = 27$ trilinear hexahedrons, as shown in Figs. 7 and 8. This model is obtained by first approximating the sphere surface with $6 \times (3 \times 3) = 54$ (curved and flat) bilinear quadrilaterals, as in Fig. 7. The sphere volume was next divided into 27 parts by connecting the corresponding vertices of the quadrilaterals by straight lines parallel to the axis of

the global rectangular co-ordinate system, as in Fig. 8. Shown in Fig. 7 are co-ordinates of three vertices which define the entire structure completely. The first-degree current approximation was adopted in all the 27 hexahedrons ($N_u = N_v = N_w = 1$, a typical subdomain approximation). With partial use of symmetry, this resulted in $N_{unkn} = 208$ and $T_{CPU} = 162.86$s. These results were compared with the analytical solution in the form of Mie's series [11]. Perfect agreement of the two sets of results can be observed.

Consider next an inhomogeneous lossy dielectric sphere, consisting of two concentric spherical layers. The radii of the boundary surfaces, expressed in electrical units, are $\beta_0 a_1 = 0.163$ and $\beta_0 a_2 = 0.314$. The equivalent relative permittivities of the inner and outer layer are $\varepsilon_{er1} = 72 - j161.78$ and $\varepsilon_{er2} = 7.5 - j8.99$, respectively. The incident plane-wave electric-field intensity is $\mathbf{E}_i = 1 \exp(j\beta_0 z)\mathbf{i}_x$ V/m. The two-layer sphere was modelled by $N_{el} = 81$ trilinear hexahedrons, of which the inner sphere (of radius a_1) was modelled by 3 × 3 × 3 = 27 hexahedrons (as in Figs. 7 and 8), and the outer layer by 6 × (3 × 3) = 54 hexahedrons so that the outer shape of the approximated entire sphere is exactly the same as in Fig. 7. The adjacent sides of all the model hexahedrons are exactly the same. The first-degree polynomial current approximation ($N_u = N_v = N_w = 1$) was adopted in all the hexahedrons. The existing symmetry was partly utilised, so that the number of hexahedrons with unknown current distribution amounted to 32, and the number of unknowns to $N_{unkn} = 520$ ($T_{CPU} \simeq 19$ min).

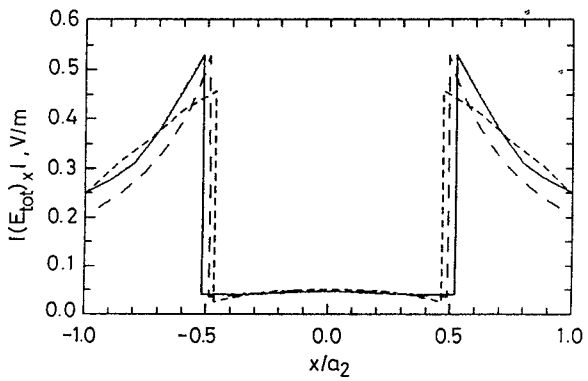

Fig. 9 *Total electric field E_{tot} inside two-layer lossy dielectric sphere*
$\beta_0 a_1 = 0.163$ (a_1 is radius of inner sphere); $\beta_0 a_2 = 0.314$; $\varepsilon_{er1} = 72$–$j161.78$; $\varepsilon_{er2} = 7.5$–$j8.99$; $\mathbf{E}_i = 1\exp(j\beta_0 z)\mathbf{i}_x$ V/m
——— analytical solution, Mie's series [6]
— — — this method, 81 elements, 520 unknowns
- - - method [6], 3375 elements, 10800 unknowns
With $|(E_{tot})_x|$ along x-axis

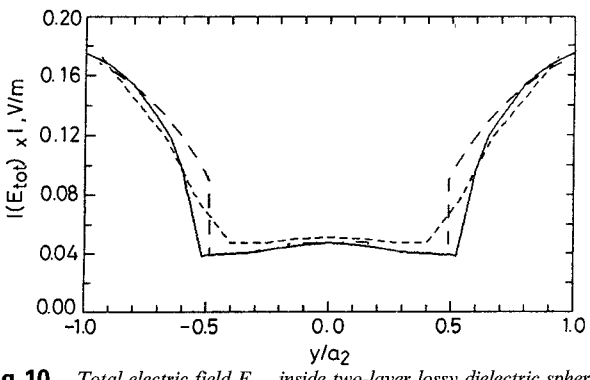

Fig. 10 *Total electric field E_{tot} inside two-layer lossy dielectric sphere*
$\beta_0 a_1 = 0.163$ (a_1 is radius of inner sphere); $\beta_0 a_2 = 0.314$; $\varepsilon_{er1} = 72$–$j161.78$; $\varepsilon_{er2} = 7.5$–$j8.99$; $\mathbf{E}_i = 1\exp(j\beta_0 z)\mathbf{i}_x$ V/m
——— analytical solution, Mie's series [6]
— — — this method, 81 elements, 520 unknowns
- - - method [6], 3375 elements, 10800 unknowns
With $|(E_{tot})_x|$ along y-axis

Shown in Figs. 9, 10 and 11 are the results for individual components of the total electric-field vector $\mathbf{E}_{tot}$ inside the sphere, along the x- and y-axis. The results obtained by the proposed entire-domain method were compared with the analytical results obtained by using Mie's series [6], and with numerical results obtained by a subdomain method [6] (10800 unknowns and T_{CPU} = 325 min on a VAX 3100/76 workstation). Good agreement of the three sets of results is observed from Figs. 9, 10 and 11, although the present method was utilised in its most unfavourable, subdomain form, with about 1/20 unknowns when compared with the subdomain method from [6].

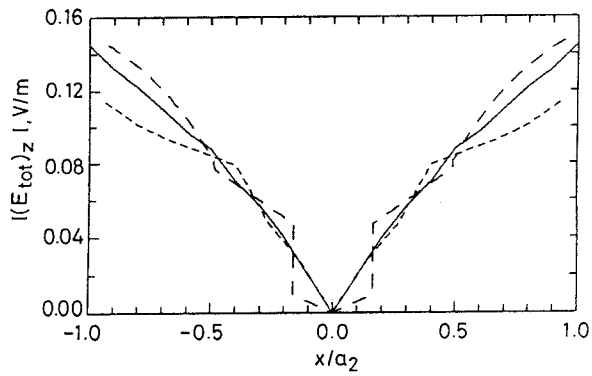

Fig. 11 *Total electric field E_{tot} inside two-layer lossy dielectric sphere*
$\beta_0 a_1 = 0.163$ (a_1 is radius of inner sphere); $\beta_0 a_2 = 0.314$; $\varepsilon_{er1} = 72$–$j161.78$; $\varepsilon_{er2} = 7.5$–$j8.99$; $\mathbf{E}_i = 1\exp(j\beta_0 z)\mathbf{i}_x$ V/m
——— analytical solution, Mie's series [6]
— — — this method, 81 elements, 520 unknowns
- - - method [6], 3375 elements, 10800 unknowns
With $|(E_{tot})_z|$ along x-axis

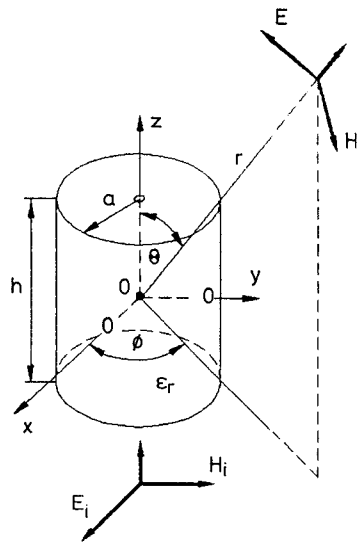

Fig. 12 *Homogeneous dielectric cylindrical scatterer in field of plane wave*

As the last example, consider a homogeneous lossless dielectric cylinder of relative permittivity $\varepsilon_r = 2$. Let the cylinder be excited by a plane wave as shown in Fig. 12 and $h = 2a = 0.7733\lambda_0 = 1.094\lambda_d$. It can be shown that this is a resonant scatterer [11]. The cylinder in Fig. 12 was approximated by only two equal trilinear hexahedrons with flat sides ($N_{el} = 2$). The cross-section of this approximation is sketched in Fig. 13. In both hexahedrons it was adopted that $N_u = 4$, $N_v = 2$ and $N_w = 4$ (see Fig. 13 for reference directions of the local co-ordinates u, v and w). Symmetry with respect to the plane $y = 0$ was utilised, so that the total number of unknowns amounted to $N_{unkn} = 200$, and the CPU time was $T_{CPU} = 47.35$s.

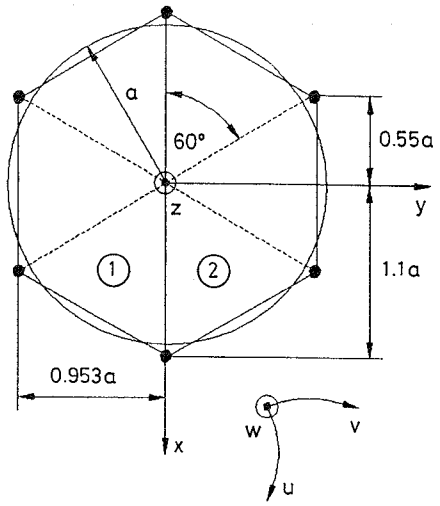

Fig. 13 *Cross-section of geometrical model of scatterer in Fig. 12 constructed from two trilinear hexahedrons*

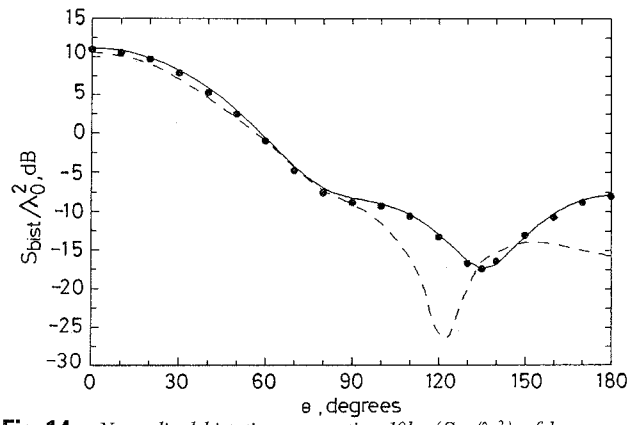

Fig. 14 *Normalised bistatic cross-section $10\log(S_{bist}/\lambda_0^2)$ of homogeneous lossless resonant dielectric cylinder for various θ in plane $\phi = 0°$*
See Fig. 12, $\varepsilon_r = 2$; h = $0.7733\lambda_0$; a = h/2
——— this method, 2 elements, 200 unknowns
• • • surface PMCHW formulation [12] (results from [11])
– – – FEM/MOM, EFIE formulation [11]

Shown in Fig. 14 is the normalised bistatic scattering cross-section, S_{bist}/λ_0^2, of the dielectric cylinder, in plane $\phi = 0°$. The results obtained by the proposed entire-domain method are compared with the results from [11] obtained by the method proposed in [12], a surface PMCHW-formulation for bodies of revolution (BOR). Excellent agreement is observed between the results obtained by the two methods.

Note that this example may be considered as a numerical evidence that the proposed method yields stable results for resonant dielectric bodies as well. Namely, it is well known that some methods do not guarantee a unique solution of resonant scatterers. To illustrate this, shown in Fig. 14 are the results from [11] obtained by the hybrid FEM/MOM method for BOR in the EFIE formulation, which are in large discrepancy with those obtained by both the proposed method and that from [12]. On the other hand, the results obtained also by the method from [11], but in the symmetrical, combined EFIE/MFIE formulation (the most preferable formulation of the method), are found to be in very good agreement with the two sets of accurate results presented in Fig. 14, and therefore are not shown.

5 Conclusion

The paper presents a novel, entire-domain, method for the analysis of (possibly lossy) dielectric scatterers of arbitrary shape and inhomogeneity. Basically, it is founded on using trilinear hexahedrons for the geometrical approximation of a scatterer, three-dimensional entire-domain polynomial functions of local parametric, in general nonorthogonal, co-ordinates for the approximation of the equivalent electric displacement vector, and the Galerkin test procedure for solving the volume two-potential integral equation.

The method is very accurate, efficient and reliable. It enables the analysis of (lossy) dielectric scatterers exceeding medium electrical size on even standard personal computers, in very reasonable amount of CPU time. In all cases considered, the results obtained by the proposed method are in very good agreement with those from other sources. However, the proposed method requires much less unknowns (for one and even two orders of magnitude) when compared with any available, subdomain, method.

The proposed method does not possess the convolution structure of the solution. Therefore there is no (direct) way to perform the conjugate gradient FFT technique to speed up the computation, which is possible with some subdomain methods. Nevertheless, numerical examples (some of which are presented in this paper) have demonstrated that the total CPU time needed for solving a problem with approximately equal accuracy greatly favours the present method also over those subdomain methods which do use this technique.

6 References

1 SCHAUBERT, D.H., WILTON, D.R., and GLISSON, A.W.: 'A tetrahedral modeling method for electromagnetic scattering by arbitrarily shaped inhomogeneous dielectric bodies', *IEEE Trans.*, 1984, **AP–32**, (1), pp. 77–85
2 TSAI, C.-T., MASSOUDI, H., DURNEY, C.H., and ISKANDER, M.F.: 'A procedure for calculating fields inside arbitrarily shaped, inhomogeneous dielectric bodies using linear basis functions with the moment method', *IEEE Trans.*, 1986, **MTT–34**, (11), pp. 1131–1139
3 SU, C.C.: 'The 3-D algorithm of solving the EFIE using face-centered node points, CGM and FFT'. Proceedings of 6th ICAP, York, April 1989, pp. 489–491
4 SARKAR, T.K., ARVAS, E., and PONNAPALLI, S.: 'Electromagnetic scattering from dielectric bodies', *IEEE Trans.*, 1989, **AP–37**, (5), pp. 673–676
5 RUBIN, B.J., and DAIJAVAD, S.: 'Radiation and scattering from structures involving finite-size dielectric regions', *IEEE Trans.*, 1990, **AP–38**, (11), pp. 1863–1873
6 ZWAMBORN, A.P.M.: 'Scattering by objects with electric contrast'. PhD dissertation, Delft University Press, ISBN 90–6275–691–3/CIP, Delft, 1991
7 ZWAMBORN, P., and VAN DEN BERG, P.M.: 'The three-dimensional weak form of the conjugate gradient FFT method for solving scattering problems', *IEEE Trans.*, 1992, **MTT–40**, (9), pp. 1757–1766
8 POPOVIĆ, B.D., and NOTAROŠ, B.M.: 'Entire-domain polynomial approximation of volume currents in the analysis of dielectric scatterers', *IEE Proc.-Microw. Antennas Propag.*, 1995, **142**, (3), pp. 207–212
9 HARRINGTON, R.F.: 'Field computation by moment methods' (Macmillan, New York, 1968)
10 NOTAROŠ, B.M.: 'Numerical analysis of dielectric bodies of arbitrary shape and inhomogeneity in the electromagnetic filed' (in Serbian). DSc thesis, Department of Electrical Engineering, University of Belgrade, 1995
11 HOPPE, D.J., EPP, L.W., and LEE, J.-F.: 'A hybrid symmetric FEM/MOM formulation applied to scattering by inhomogeneous bodies of revolution', *IEEE Trans.*, 1994, **AP–42**, (6), pp. 798–805
12 HUDDLESTON, P.L., MEDGYESI-MITSCHANG, L.N., and PUTNAM, J.M.: 'Combined field integral equation formulation for scattering by dielectrically coated conducting bodies', *IEEE Trans.*, 1986, **AP–3**, (4), pp. 510–520